

## Local induction of spatio-temporal chaos

G. Baier, A. Ramírez, I. Amaro, and M. Müller  
*Facultad de Ciencias, Universidad Autónoma del Estado de Morelos,  
 62210 Cuernavaca, Morelos, México*  
*e-mail: baier@servm.fc.uaem.mx*

Recibido el 3 de diciembre de 2004; aceptado el 14 de junio de 2005

A periodic perturbation of one excitable system causes a symmetry-breaking instability in two reversibly coupled neighbors. The result is applied to a two-dimensional extended system. Tuning of the local perturbation frequency causes a regular target pattern to switch first to circular chaotic waves and then to chaotic wave fragments. Thus a global order-disorder transition can be induced by local control in an otherwise homogeneous medium.

*Keywords:* Spatio-temporal chaos; order-disorder transition; local control.

Una perturbación periódica de un sistema excitable causa un rompimiento de simetría en dos osciladores acoplados reversiblemente. El resultado es aplicado a un sistema extendido en dos dimensiones espaciales. Ajustando la frecuencia de la perturbación local, se cambia un patrón regular de ondas circulares primero a ondas circulares caóticas y después a fragmentos de ondas caóticas. En consecuencia, una transición global orden-desorden se puede inducir bajo control local en un medio homogéneo.

*Descriptores:* Caos espacio-temporal; transición orden-desorden; control local.

PACS: 05.45.Ac; 05.45.Jn; 05.45.Xt

Order-disorder transitions in biological excitable media, like the onset of heart fibrillation [1] or the cessation of epileptic seizures (see *e.g.* Ref. 2), appear to occur spontaneously. There is no evidence of global changes, either of global parameters or of global external perturbations. The crucial factors that could account for these transitions are thus still unknown (see Refs. 1 and 2 in the case of fibrillation and epilepsy, respectively). A conceptually simple hypothesis is that both the regular and the irregular patterns are controlled by the activity of the same local pacemaker. In principle, order-disorder transitions could then be due to altered dynamics of this pacemaker, *i.e.* due to *local* parameter changes. So far, however, no explicit model has been available for studying such a hypothesis.

In autonomous excitable systems, transitions to spatio-temporal chaos have been observed experimentally as a function of the overall experimental conditions. Accordingly, the proposed explanations employed a global change (a change in many or all sites) in at least one model parameter. Examples are the models to explain

- i) chaotic patterns in the Belousov-Zhabotinsky reaction [3];
- ii) the spiral break-up during the CO oxidation on platinum crystals [4];
- iii) the transition to heart fibrillation [5]; and
- iv) the dynamics of epileptic seizures [6].

It is also possible to experimentally induce transitions to spatio-temporal chaos by external perturbations [7], or by feedback perturbations [8], but in all cases the whole system (or a large part of it) has to be perturbed and thus, again,

global influences are responsible for the transition. Unless (static) spatial heterogeneities are introduced in to the models, parameters have to be adjusted globally in the chaotic domain, to obtain spatio-temporal chaos [9].

An exception is the suggested mechanism for pattern transitions in frog eggs, where an *excitable* chaotic system was introduced [10]. This model system undergoes global order-disorder transitions as a function of local periodic perturbations. However, the chaotic solution was composed only of subthreshold oscillations, and did not contain any suprathreshold excitation. (Here and later on the term “subthreshold” means that the internal excitation threshold of an excitable system is not crossed. In contrast, if the threshold is crossed, the term suprathreshold is used. See *e.g.* Ref. 11 for details.)

To show that complex pattern transitions can indeed be under the control of nothing but the pacemaker dynamics, we first investigate how spatio-temporally non-synchronized chaos can be induced in a prototype of three coupled, excitable units. Then we apply the results to a spatially extended model and demonstrate transitions from regular to chaotic excitation patterns as a function of the frequency of a local periodic forcing.

The FitzHugh-Nagumo (FHN) model is used in the following form:

$$\begin{aligned} \frac{dX_1}{dt} &= X_1(a - X_1)(X_1 - 1) - Y_1 + I_a \\ &\quad + D_X(X_2 + X_3 - 2X_1) + A \sin(t/T) \\ \frac{dY_1}{dt} &= bX_1 - cY_1 + D_Y(Y_2 + Y_3 - 2Y_1) \end{aligned}$$

$$\begin{aligned}
 \frac{dX_2}{dt} &= X_2(a - X_2)(X_2 - 1) - Y_2 + I_a \\
 &\quad + D_X(X_1 + X_3 - 2X_2) \\
 \frac{dY_2}{dt} &= bX_2 - cY_2 + D_Y(Y_1 + Y_3 - 2Y_2) \\
 \frac{dX_3}{dt} &= X_3(a - X_3)(X_3 - 1) - Y_3 + I_a \\
 &\quad + D_X(X_1 + X_2 - 2X_3) \\
 \frac{dY_3}{dt} &= bX_3 - cY_3 + D_Y(Y_1 + Y_2 - 2Y_3) \tag{1}
 \end{aligned}$$

In the absence of external perturbations ( $A=0$ ), and with parameters  $a=0.14$ ,  $b=0.01$ ,  $c=0.02$ , each isolated unit ( $D_X = D_Y = 0$ ) has one stable focus for  $I_a < 0.044$ . At  $I_a \approx 0.045$  a subcritical Hopf bifurcation occurs. At this point the region of bistability (coexistence of limit cycle and fixed point) that started at  $I_a \approx 0.044$  ceases to exist and the stable limit cycle is the only attractor in phase space. By further analyzing the bifurcation behavior as a function of other parameters, we found that with the given set of parameters the system is located near the region of supercritical Hopf bifurcation in parameter space (*i.e.* no bistability between limit cycle and fixed point).

In the coupled system, the three oscillators are arranged in a triangle with reversible mutual couplings. Oscillators 2 and 3 are symmetric with respect to the perturbation in oscillator 1: they receive the same positive input  $D_X X_1$ . If their initial conditions are chosen to be identical, they will therefore behave identically. In this case the system reduces to two oscillators. The perturbed two-oscillator subsystem shows a large variety of quasiperiodic, complex periodic, and chaotic solutions as a function of the perturbations parameter, comparable to the case of a single perturbed nonlinear oscillator [11].

Next, we shall consider the full system (Eq. (1) with non-identical initial conditions in oscillators 2 and 3). Fig. 1 is a two-dimensional parameter scan of forcing amplitude and frequency. The two features evaluated are

- 1) whether the system generates spikes (*i.e.* whether or not variables  $X$  cross a threshold after they have settled on the attractor); and
- 2) whether oscillators 2 and 3 are synchronized or not.

It should be noted that in this range of forcing frequencies, the system's threshold minimum is at amplitudes  $A < 0.01$  for sinusoidal forcing, *i.e.* the amplitudes in Fig. 1 are above this minimum. In the chosen area of the parameter plane, there is an island of non-spiking behavior (the white region), adjacent to which is a region of desynchronized spiking (black region). The rest of the plane (grey) exhibits synchronized spiking (periodic or chaotic). Numerically we did not observe desynchronized behavior in the non-spiking regions.

Thus, in the black area, a difference in initial conditions of oscillators 2 and 3 is sufficient to break their spatial symmetry dynamically and observe desynchronized behavior. The scan Fig. 1 was found to be qualitatively independent of the choice of initial conditions. At the borders, particularly between the black and grey area, there is a thin region where numerically it could not be decided whether there exists a region of bistability because transients tend to be very long. However, we verified that the location of the border does not change depending on the choice of initial conditions or on the choice of transient time (*i.e.* the part of the dynamics that is not evaluated).

We calculated bifurcation diagrams as a function of forcing period  $T$  in the plane of Fig. 1. At constant forcing amplitude  $A=0.075$ , a window of chaotic behavior ( $7.4 < T < 8.6$ ) is hemmed in by periodic solutions of period 1 and period 2, respectively. Comparing the results for maxima of  $X_2$  with those obtained for differences of maxima ( $X_2 - X_3$ ) reveals two regions of synchronization,  $7.4 < T < 7.75$  and  $8.4 < T < 8.6$ . Both lie within the chaotic window, *i.e.* they occur in the presence of a positive Lyapunov exponent. In the intermediate region ( $7.75 < T < 8.4$ ), oscillators 2 and 3 are not only chaotic but also desynchronized. Fig. 2 displays Poincaré cross-sections of the synchronized and the desynchronized chaotic attractor projected on to the  $X_2/X_3$  plane. The synchronized dynamics (Fig. 2a) consequently stays on the diagonal. The desynchronized dynamics (Fig. 2b) shows increased density of intersection points near the diagonal, but otherwise covers a square area in a multiply folded sheet pattern. Before applying the criterion of differences between

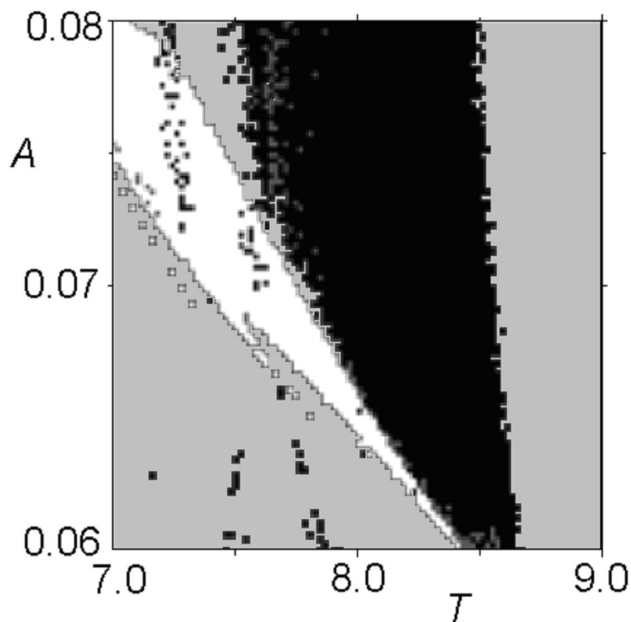


FIGURE 1. Scan of parameter plane  $T/A$  in Eq. (1). White: no excitation, synchronized. Grey: excitation, synchronized. Black: excitation, desynchronized. Parameters:  $a=0.14$ ,  $b=0.01$ ,  $c=0.02$ ,  $I_a=0.042$ ,  $D_X=0.08$ ,  $D_Y=0$ . Synchronization is defined as  $(X_3 - X_2) < 0.01$  after a transient time of 500,000 time units.

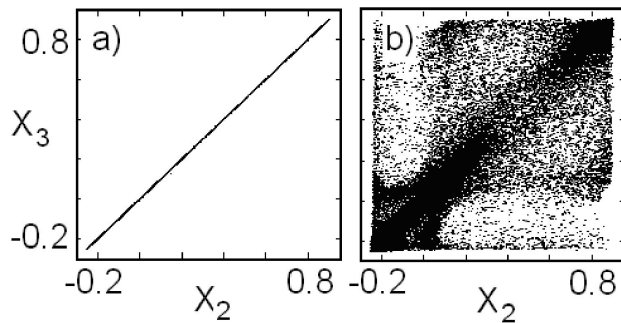


FIGURE 2. Return maps constructed from maxima of the two symmetrically equivalent oscillators 2 and 3. a)  $T=8.45$ ; b)  $T=8.35$ .  $A=0.075$ , other parameters as in Fig. 1.

maxima, we verified that it actually represents synchronization of the attractors, and that the number of maxima found with this criterion in the nonsynchronized dynamics is vanishingly small.

Two aspects of the result in Fig. 2 deserve discussion. First, as deterministic chaos requires the instability of periodic orbits, it is normally found in the self-oscillating region of parameter space [11]. The reason our excitable system (with non-oscillatory resting state) can become chaotic under periodic perturbation is its location near the border to supercritical Hopf bifurcation in parameter space. And secondly, calculating spectra of Lyapunov exponents for Eq. (1), we find that the sum of the three largest exponents fulfills the Kaplan-Yorke condition [12] for dimension increase for both the synchronized and the desynchronized dynamics, *i.e.* the dimension is larger than 3, whereas a dimension less than 3 is expected for dynamics that does not fulfill the condition. Thus, neither a new source of exponential divergence nor a sudden increase of the fractal dimension can explain the transition between the two types of dynamics.

Synchronization-desynchronization transitions related to the one in Fig. 2 were reported in coupled chaotic oscillators as a function of coupling strength [13]. Similar to these cases, in our system we find a sudden transversal instability of the synchronized state accompanied by a change of sign of the transverse Lyapunov exponent [14], with typical on-off intermittent behavior near the instability [15]. A difference is that in our case, there is no chaos prior to external perturbation, either in the individual unit or in the autonomous coupled system. Therefore, we assume that the creation of chaos in the vicinity of a supercritical Hopf bifurcation plays an important role for the transition to occur. Once the chaos is induced, the transversal instability occurs as in coupled chaotic systems.

Notably, the chaos is created by the perturbation of a unit that is not considered in the symmetry-breaking. In this new prototype, the *source* of the symmetry-breaking instability and its measurable effect are separated from each other. As each affected unit (oscillators 2 and 3) in turn is a possible source of this instability, there is no reason to assume that the symmetry-breaking is restricted to immediate neighbors of the perturbed unit in spatially extended systems.

The question is whether the induced chaos in oscillators 2 and 3 is such that it can in turn induce an equivalent symmetry-breaking transition in other neighbors. If so, the instability might invade a system composed of a large number of coupled units. This hypothesis was tested using one perturbed excitable unit (like oscillator 1) surrounded by two rings, an inner ring of 6 and an outer ring of 12 diffusively coupled FHN units in a hexagonal arrangement (*i.e.* the central unit and the inner ring having 6 nearest neighbors, and the outer ring having 3 and 4 nearest neighbors). Under conditions as in the three-unit prototype, a transition from regular to chaotic excitations, and subsequently the symmetry-breaking of the chaotic solution, is observed as a function of forcing frequency. Both transitions occur in the inner as well as in the outer ring. This observation was also repeated with the perturbation placed in a position other than the central one. The corresponding instabilities are thus able to propagate to more distant units. We demonstrate this in an extended system of diffusive coupled FHN units.

The chosen system has two spatial dimensions, zero-flux boundaries, and randomly chosen initial conditions. In the absence of an external perturbation, the system settles into its excitable resting state, a stable focus. A periodic perturbation (as in oscillator 1 of Eq. (1)) is applied to only one of the units in the plane. We analyze the system's patterns as a function of the forcing period for constant amplitude  $A=0.075$ . The observed sequence of patterns for decreasing period  $T$  is:

- i) a window of period 1 excitation waves where each period in the perturbation causes one wave ( $9.0 < T < 10.0$ );
- ii) a window of chaotic excitation wave patterns ( $7.9 < T < 9.0$ ); and
- iii) a window with no excitation waves (no suprathreshold oscillations at a distance of more than 2 oscillators from the perturbation point) in  $6.0 < T < 7.9$ .

Figure 3 displays snapshots of the system with perturbation parameters in the chaotic window.

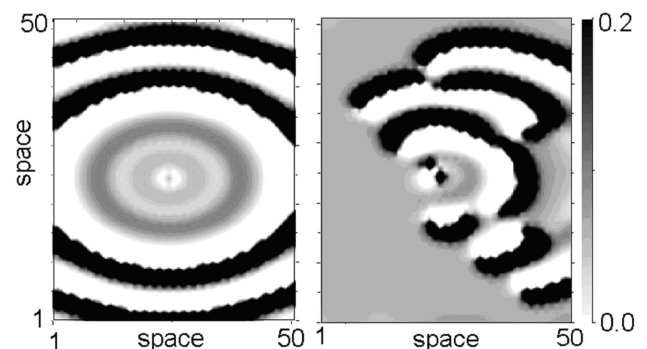


FIGURE 3. Snapshots of chaotic patterns in the periodically perturbed hexagonal 2D system of  $50 \times 50$  FHN units as in Eq. (1) with pacemaker in oscillator [25,25]. a)  $T=8.9$ . b)  $T=8.6$ .  $D_X=0.012$ ,  $D_Y=0.001$ , other parameters as in Fig. 2. Grey coding of variables  $X$  from  $-0.2$  (white) to  $0.8$  (black).

The excitation pattern in Fig. 3a is obtained for a forcing period that lies close to the period 1 regular waves. Here the circular symmetry of the waves is preserved in a “target” pattern. The amplitudes of consecutive waves are not identical, however. Notably in the picture is a so-called “missing beat”, *i.e.* a wave of small amplitude that corresponds to a sub-threshold near-harmonic oscillation of a single element (grey ring). The proximity in parameter space to the period 1 solution is recognizable in occasional “bursts”, series of up to 10 almost periodic spikes separated by non-spiking periods. Both the number of missing waves and the periods between them are irregular. In spite of the circular symmetry, the time series of all units are chaotic.

Figure 3b is a snapshot at a forcing period farther away from the period 1 solution and closer to the no-propagation window. Here, during the initial phase, the circular symmetry is broken for non-identical initial conditions of the variables. The result is a mixture of complete circular waves (rare), partial waves and small wave fragments. The time series of any chosen element is an aperiodic sequence of excitations with highly irregular inter-spike-intervals and the dynamics is deterministic chaos. In addition to the loss of correlation in time there is a loss of correlation in all spatial directions. This is the main difference from the case in Fig. 3a with circular spatial symmetry.

Both hexagonal and cubic geometries were tried to confirm the independence of the results from the particular geometry of coupling. Periodic boundary conditions in one (cylinder) or two (torus) dimensions were found to produce the same qualitative results for essentially the same parameters. One difference is that periodic boundary conditions allow chaotic wave fragments to re-enter the perturbation zone and interfere with the wave generation process. In this case, the curvature of the wave fragments no longer yields clues about the position of the pacemaker.

If all time series of individual oscillators are at hand, it is a straightforward matter to distinguish the two chaotic excitation states by comparing their symmetry. However, if only some integral measurement of the pattern is available, this is not necessarily the case. We generated artificial “electrocardiograms” from the two patterns in Fig. 3, and obtained highly irregular time series in both cases. The distinct symmetries are not discernible in such representations. This is of importance in physiological research into heartbeat and electric brain activity, where often only mean-field data (the electrocardiogram and electroencephalogram, respectively) are used for the evaluation of the dynamics.

The transition between the chaotic patterns in Fig. 3 appears to be abrupt, as in the case of the 3 oscillator system

Eq. (1). No bistability was observed numerically but, with parameters very close to the transition point, transients become long, depending on the choice of initial conditions, and therefore the possibility of a very small region of bistability may not be excluded at present. If the system is started on the period 1 attractor with regular excitation waves and parameter  $T$ , and then is shifted into the chaotic region of Fig. 3a, only the periodicity of the original pattern is destroyed. The symmetry is preserved. If, however, parameter  $T$  is switched into the chaotic region of Fig. 3b, the spatial symmetry of the original pattern is broken also. These results were confirmed with a random Gaussian distribution of bifurcation parameter  $I_a$ , creating a non-homogeneous net. Thus, a global periodic pattern in a homogeneous excitable medium close to the transition from subcritical to supercritical Hopf bifurcation can be generically switched into spatio-temporally chaotic patterns by the seemingly trivial frequency change of a local periodic perturbation.

The reverse disorder-order transition is harder to achieve. Once the system is in the chaotic state of Fig. 3b, a resetting of the parameters into the period 1 window does not necessarily mean that the system returns to period 1 waves within a finite time. The reason is that the present wave fragments keep breaking newly generated circular waves. This results in new fragments and this process can continue to hamper the restauration of the circular symmetry. Only if for a considerable time there happen to be *no* excitation waves, the local pacemaker then has a chance to restore, and thereafter maintain, a complete circular wave symmetry. One is reminded of the benefits of a defibrillator in case of fibrillation: a voltage shock is used to deliberately eliminate *all* stray excitation fragments in order to return the heart to a uniform resting state before its (natural) pacemaker can successfully resume its work.

The presented excitable system allows for locally controlled transitions from symmetric periodic to symmetric chaotic and to asymmetric chaotic patterns. It is possible to test for this novel property experimentally by introducing local pacemakers into experimental systems and scanning their frequency and amplitude. We suggest that the model offers an alternative working hypothesis for sudden transitions to fibrillation, for the dynamic reorganization of epileptic states, and possibly even for stimulus-induced order-disorder-order transitions during cognitive acts in the human brain [16].

## Acknowledgements

This work was supported by CONACyT, Mexico (project no. 40885-F). G.B. thanks Sven Sahle for the discussion.

1. R.A. Grey, A.M. Pertsov, and J. Jalife, *Nature* **392** (1998) 75; F.X. Witkowski *et al.*, *Nature* **392** (1998) 78.
2. D.F. Smith *et al.* (eds.), *An Atlas of Epilepsy* (Parthenon Publishing, New York, 1998); J. Milton and P. Jung (eds.), *Epilepsy as a Dynamic Disease* (Springer, New York, 2003).
3. O.E. Rössler and Z. Naturforsch, **31a** (1976) 1168; Y. Kuramoto, *Progr. Theor. Phys. Suppl.* **64** (1979) 346.
4. M. Bär and M. Eiswirth, *Phys. Rev. E* **48** (1993) R1635.
5. A. Panfilov and P. Hogeweg, *Phys. Lett. A* **176** (1993) 295; F.H. Fenton *et al.*, *Chaos* **12** (2002) 852.
6. M.C. Mackey and U. an der Heiden, *J. Math. Biol.* **19** (1984) 211.
7. O. Steinbock, V.S. Zykov, and S.C. Müller, *Nature* **366** (1995) 322; V. Petrov, Q. Ouyang, and H.L. Swinney, *Nature* **388** (1997) 655; A.L. Lin *et al.*, *Phys. Rev. E* **62** (2000) 3790.
8. V.K. Vanag *et al.*, *Nature* **406** (2000) 389; M. Hildebrand, H. Skødt, and K. Showalter, *Phys. Rev. Lett.* **87** (2001) 088303; I.Z. Kiss, Y. Zhai, and J.L. Hudson, *Phys. Rev. Lett.* **88** (2002) 238301.
9. A.T. Winfree, *Science* **266** (1994) 1003.
10. G. Baier, S. Sahle, J.-P. Chen, and A. Hoff, *J. Chem. Phys.* **110** (1999) 3251.
11. W. Gerstner and W. Kister, *Spiking Neuron Models* (Cambridge University Press, 2002).
12. See the chapters by K. Tomita *et al.*, in: A.V. Holden (ed.), *Chaos* (Princeton University Press, Princeton, 1986).
13. J. Kaplan and J.A. Yorke, *Lecture Notes in Mathematics* **730** (1979) 204.
14. M.G. Rosenblum, A.S. Pikovsky, and J. Kurths, *Phys. Rev. Lett.* **76** (1996) 1804; E. Mosekilde, Y. Maistrenko, and D. Postnov, *Chaotic Synchronization* (World Scientific, Singapore 2002).
15. J.C. Sommerer and E. Ott, *Nature* **365** (1993) 138; E. Ott and J.C. Sommerer, *Phys. Lett. A* **188** (1994) 39.
16. N. Platt, E.A. Spiegel, and C. Tresser, *Phys. Rev. Lett.* **70** (1993) 279.
17. E. Rodriguez *et al.*, *Nature* **397** (1999) 430.